Mannosylated nanoparticles for oral immunotherapy in a murine model of peanut allergy

Ana Brotons-Canto[a], Carlos Gamazo[a], Nekane Martín-Arbella[a], Muthanna Abdulkarim[b], Mark Gumbleton[b], Gemma Quincoces[c], Ivan Peñuelas[c], Juan M. Irache[a]

Affiliation

[a] NANO-VAC Research Group, Instituto de Investigación Sanitaria de Navarra (IdiSNA), University of Navarra, 31008, Pamplona, Spain.

[b] School of Pharmacy and Pharmaceutical Science, Cardiff University, Cardiff, UK.

[c] Radiopharmacy Unit, Department of Nuclear Medicine, Clinica Universidad de Navarra, University of Navarra, Spain.

Corresponding author:

Prof. Juan M. Irache
Dep. Pharmacy and Pharmaceutical Technology
University of Navarra
C/ Irunlarrea, 1
31080 – Pamplona
Spain
Phone: +34948425600
Fax: +34948425619
E-mail: jmirache@unav.es

Abstract

Peanut allergy is one of the most prevalent and severe of food allergies with no available cure. The aim of this work was to evaluate the potential of an oral immunotherapy based on the use of a roasted peanut extract (PE) encapsulated in nanoparticles with immunoadjuvant properties. For this, a polymer conjugate formed by the covalent binding of mannosamine to the copolymer of methylvinyl ether and maleic anhydride was firstly synthetized and characterized. Then, the conjugate was used to prepare nanoparticles with an important capability to diffuse through the mucus layer and reach, in a large extent, the intestinal epithelium, including Peyer's patches. Their immunotherapeutic potential was evaluated in a model of pre-sensitized CD1 mice to peanut. After completing therapy, mice underwent an intraperitoneal challenge with PE. Nanoparticle-treatment was associated with both less serious anaphylaxis symptoms and higher survival rates than control, confirming the protective effect of this formulation against the challenge.

Keywords: formulation; immunotherapy; mucosal immunization; oral drug delivery; nanoparticles; protein delivery; vaccine adjuvants

1. Introduction

Food allergy is a serious and growing problem. For peanut allergic patients, they must maintain a strict allergen-free diet and carry emergency medication (i.e., epinephrine auto-injectors) to treat anaphylactic symptoms following accidental exposure [1]. In spite of improvements in industrial cleaning procedures and food labelling, accidental exposures continue to be the leading cause of anaphylaxis [2]. Particularly for young patients, the persistent fear to accidental exposures as well as the life-threatening reactions significantly disrupts their social and educational activities [3,4] This profoundly impairs health-related quality of life, to an extent greater than that seen in chronic conditions such as diabetes mellitus [5].

Oral immunotherapy (OIT) has been suggested as a promising therapy for food allergy. OIT is based on the delivery of increasing doses of allergens with the objective of inducing desensitization and/or tolerance [6]. The exact mechanism underlying desensitization is not well understood. Nevertheless, from an immunological point of view, OIT would induce allergen-specific IgG4 antibodies, reducing at the same time specific IgE [7]. IgG4 acts as a blocking antibody for specific IgE, inhibiting IgE-mediated mast cell activation and degranulation [8]. This activation of mast cells produces the release of vasoactive amines and cytokines, responsible for the symptoms associated to allergic reactions.

Different clinical trials have provided evidences that OIT can effectively desensitize a majority of individuals to a food allergen; although, the safety and tolerability of the conventional treatments continue to limit its use [9-11]. Recently, in order to improve the efficacy and safety of conventional OIT, the use of polymer nanoparticles as allergen

delivery systems has been proposed [12]. In principle, these devices may offer the following advantages: (i) protection of the loaded allergen from its premature degradation by the harsh conditions of the gut [13], (ii) co-encapsulation of immunomodulators to boost appropriate tolerogenic adaptive immune responses to allergens [14,15], and (iii) facilitate the presentation of the allergen to the GALT (gut associated lymphoid tissue) and promote a protective response [16,17].

However, when polymer nanoparticles are orally administered, they are faced to the protective mucus layer that highly hampers their arrival to the intestinal epithelium [18,19]. In fact, the mucus layer acts a as a barrier in which nanoparticles remain trapped by mucoadhesive forces and, thus, minimising their interaction with the immune cells localized in the intestinal epithelium [20]. Among others, hydrophobic interactions between the surface of nanoparticles and hydrophobic domains of glycoproteins constituting the mucus play a major role in the mucoadhesion phenomenon [21]. In order to minimize this drawback, different approaches have been proposed including the use of “slippery” nanoparticles. These nanocarriers, with mucus-permeating properties, may be obtained by the coating or functionalization of nanoparticles with hydrophilic compounds, such as poly(ethylene glycols) [22] or poloxamers [23]. Another interesting approach may be the functionalization of these nanoparticles with hydrophilic compounds with the capability of recognizing and binding to specific receptors localized on the surface of particular intestinal cells. In this context, the use of mannose modified nanoparticles may be a good strategy to target intestinal dendritic cells and M-cells of Peyer’s patches [24,25].

The aim of this work was the preparation and characterization of mannosamine-modified nanoparticles as carriers for a peanut extract containing the main allergens. In the recent past, the nanoencapsulation of a peanut extract containing the main allergenic proteins (PE) in nanoparticles, from the copolymer of methyl vinyl ether and maleic anhydride (Gantrez® AN), displayed an important capability to induce a balanced Th1 and Th2 antibody response after one single dose [26]. Specifically, mice treated with these nanoparticles displayed high levels of IFN-ɣ and IL-10 with lower pro-Th2 cytokines (IL-4, IL-5, IL-6) and reduced specific IgE levels compared to control [26]. In the present work, the capability of nanoparticles based in a polymer conjugate between Gantrez® AN and mannosamine to carry this peanut extract and to offer protection against anaphylaxia in a peanut sensitized mice model was evaluated. Mannosamine was selected in order to improve the immunoadjuvant properties of Gantrez® AN [27] due to their capability to specifically bind and activate immune cells (i.e., dendritic cells and macrophages) [28,29].

2. Methods

2.1. Materials

Poly(methyl vinyl ether-co-maleic anhydride) or poly(anhydride) (Gantrez® AN 119) was supplied by Ashland, (Ashland, USA). Peanut extract was kindly provided by Diater® Laboratories SA (Madrid, Spain). Ethanol and rose Bengal were provided by Panreac (Barcelona, Spain). Acetone was obtained from (VWR-Prolabo). Cholera toxin, D-mannitol, D-mannosamine and Tween 20 were from Sigma-Aldrich (Germany). Lumogen® F red 305 was from Kremer (Aichstetten, Germany). Tissue-Tek® OCT

compound was obtained from Sakura (Alphen, Netherlands) 4´, 6-diamidino-2-phenylindole (DAPI) was obtained from Biotium Inc. (Hayward, CA). Micro-BCA™ Protein Assay Reagent Kit was from Pierce® (Rockford, USA). Veratox Peanut Kit was from Neogen (Lansing, MI, USA) and CAPITAN MANI® soft peanut butter was from Alimentación Varma, S.L. (Alcobendas, Madrid). Sodium hydroxide (NaOH) was from Scharlau (Spain).

PLGA nanoparticles (PLGA-NP) were kindly supplied by Nanomi B.V. (The Netherlands). These nanoparticles displayed a mean size of 161 nm with a polydispersity index of 0.03 and negative zeta potential of -29 mV.

2.2. Peanut extract dialysis

Prior the encapsulation in nanoparticles, the roasted peanut extract was dispersed in deionised water and transferred to a dialysis bag (MWCO 3500). The bag was introduced into a vessel with 15 mL water and maintained under agitation for 48 h at 8°C. Finally, the bag contents were transferred to vials and lyophilized in a Genesis 12 EL apparatus (Virtis, USA). For experimental studies, only the dialyzed peanut extract (PE) was used. The extract was characterized by SDS-PAGE and proteomic analysis in order to confirm the presence of the main allergenic proteins (Ara h1, Ara h2, Ara h3, Ara h5-8 and oleosins).

2.3. Preparation and characterization of Gantrez® AN-mannosamine conjugate (GM)

The conjugate was formed by the covalent binding of mannosamine to the anhydride groups of the polymer backbone. For this purpose, 1 g Gantrez® AN [poly(anhydride)] was dissolved in 120 mL acetone. Then, 50 mg mannosamine were added and the mixture was heated at 50 ºC, under magnetic agitation at 400 rpm for 3 h. Then, the mixture was filtered through a pleated filter paper and the organic solvent was eliminated under reduced pressure in a Büchi R-144 apparatus (BÜCHI Labortechnik AG, Flawil, Switzerland) until the conjugate was totally dry. Finally, the resulting powder was stored at room temperature in a hermetically sealed container until use.

For the characterization, GM was analysed by infrared spectroscopy, elemental analysis, ^{1}H-NMR and titration. The amount of mannosamine bound to the poly(anhydride) was estimated by the o-phthalaldehyde (OPA) method [30]. More details about the characterization of GM are provided in the "Supplementary Material" section.

2.4. Preparation of nanoparticles

2.4.1. Preparation of unloaded nanoparticles (GM-NP)

For the preparation of unloaded nanoparticles, 400 mg GM polymer was dissolved in 20 mL acetone to form solution 1. Then 40 mL of a hydroalcoholic mixture (10 mL water and 30 mL ethanol) containing 80 µL calcium chloride (0.8% w/v) was added to solution 1 where GM-NP nanoparticles were formed under continuous magnetic stirring. The organic solvents were evaporated under reduced pressure (Rotary evaporator, Büchi R-144, Switzerland) and the nanosuspensions were ultracentrifuged (Sigma 3K30 Rot. 12150-H, UK) at 4ºC and 40,000 x g for 20 minutes. Finally, the resulting batch of pellets was dispersed in 40 mL 2% mannitol solution and dried by spray-drying in a Büchi Mini

Spray Drier B-290 apparatus (Büchi Labortechnik AG, Switzerland). The parameters for spray drying were: inlet temperature of 90 ºC, outlet temperature of 60 ºC, spray-flow of 600 mL/h, and aspirator at 100% of the maximum capacity. These nanoparticles were named GM-NP.

As controls, nanoparticles based on Gantrez ® AN (NP) were prepared as described previously [31].

2.4.2. Preparation of peanut extract-loaded nanoparticles

Peanut extract-loaded nanoparticles were prepared by the dissolution of 400 mg GM in 20 mL acetone. Then, 12 mg of the peanut extract (previously resuspended in 100 µL of purified water adjusted to a pH 3 with HCl 0.1N) was added to this solution and incubated, under agitation, for 45 minutes. Nanoparticles were obtained, purified and dried as described above. The resulting nanoparticles were identified as PE-GM-NP.

2.4.3. Preparation of fluorescently labelled nanoparticles

Nanoparticles were fluorescently labelled by the encapsulation of Lumogen® F Red 305. Briefly, 4 mg Lumogen Red was dissolved in a solution of acetone containing GM or Gantrez® AN polymer prior to the formation of the nanoparticles as described above. The resulting nanoparticles were purified and dried as described above.

2.5. Physico-chemical characterization of nanoparticles

For the characterization of nanoparticles, their size and zeta potential were determined by photon correlation spectroscopy (PCS) and electrophoretic laser Doppler anemometry, respectively, using a Zetaplus apparatus (Brookhaven Inst. Corp.). The yield of the preparative process of nanoparticles was calculated by gravimetry,[31]

whereas the amount of peanut encapsulated into nanoparticles was measured by using the bicinchonic acid method (microBCA). The surface hydrophobicity of unloaded and loaded nanoparticles was evaluated by the Rose Bengal test as previously described [32], with some minor modifications. Finally, the stability of nanoparticles was evaluated by measuring the turbidity changes as a function of time in buffer solutions with different pH value corresponded to simulated gastric and intestinal fluids SGF and SIF (i.e., pH 1.2 and 6.8, respectively). More details about these studies are provided in "Supplementary Material".

2.6. In vitro release

The release studies were performed under sink conditions by using simulated gastric (SGF) and intestinal fluids (SIF), supplemented with Tween 20 (1% w/v). For these purpose, Float-A-Lyzer devices with a MWCO of 300 kDa (Spectrum Labs, Breda, The Nederlands) were used. First, the dialysis bags were washed with ethanol 10% for 10 min and secondly, with water. The bags were filled with 96 mg formulation dispersed in 5 mL SGF and then, placed into a vessel containing 660 mL SGF. The vessel was maintained under magnetic agitation and 200 µL samples were withdrawn at fixed time intervals and replaced with equal volumes of SGF. After two hours of incubation in SGF, the bags were transferred to a second vessel with 660 mL SIF. Again, at fixed times, 200 µL were withdrawn and replaced with free SIF.

The amount of PE released from nanoparticles was quantified with a sandwich enzyme-linked immunosorbent assay (ELISA) kit for peanut allergy (Veratox®, Neogen, Scotland, UK).

2.7. In vitro evaluation of nanoparticles diffusion in mucus

The diffusion of nanoparticles through porcine intestinal mucus barrier was measured by the Multiple Particle Tracking (MPT) technique to assess the permeation of particles through mucus barrier [33]. MPT technique involves using of epifluorescence microscopy to capture videos of particles' movement within the mucus sample followed by tracking of particles trajectories of hundreds of individual particles within the mucus matrix [34]. Measuring of particles' displacements enable us to calculated diffusion coefficients of nanoparticles <Deff>. Diffusion of particles in water (Dº) were calculated by Stoke-Einstein equation. The relative efficiency of nanoparticles diffusion (%<Deff>/ D° ratio) was calculated for comparison between particles restricted diffusion through mucus versus free movement in water. The "Supplementary Material" section describes in detail these studies.

2.8. Gastro-intestinal transit studies with radiolabelled nanoparticles

Prior to in vivo studies, nanoparticles were labelled with technetium-99m by reduction with stannous chloride as described previously [35]. All procedures were performed following a protocol previously approved by the "Ethical and Biosafety Committee for Research on Animals" at the University of Navarra in line with the European legislation on animal experiments. These studies were carried out in male Wistar rats weighing 250-300 g (Harlan, Barcelona, Spain). Animals were briefly stunned with 2% isoflurane gas (flow of oxygen of 0.2 L/min) for administration of nanoparticles by oral gavage, and then quickly awakened. Each animal received a single dose (1 mL) of nanoparticles (1

mCi; 0.8-1.0 mg with radiolabelled nanoparticles that were completed with up to 10 mg with unlabelled nanoparticles). For analysis, the animals were anaesthetised with 2% of isoflurane gas (flow of oxygen of 0.2 L/min) and placed in prone position on the gamma camera (Symbia T2 Truepoint; Siemens Medical System, USA). SPECT-CT images were acquired for 25 minutes, with the following parameters for SPECT: 128 x 128 matrix, 90 images, 7 images per second and CT: 110 mAs and 130 kV, 130 images, slice thickness 3 mm Fused images were processed using the Syngo MI Applications True D software.

2.9. Biodistribution of nanoparticles within the gut

These studies were carried out using a protocol described previously [22] with minor modifications, after approval by the "Ethical and Biosafety Committee for Research on Animals" at the University of Navarra in line with the European legislation on animal experiments. Briefly, male Wistar rats (average weight 225 g; Harlan, Barcelona, Spain) were placed in metabolic cages and fasted overnight with free access to water. All animals received orally 10 mg of fluorescently labelled nanoparticles dispersed in 1 mL water. Then, after 2 hours the animals were sacrificed by cervical dislocation and the gut was removed. Different portions of the gut were collected, cleaned with PBS, stored in the tissue proceeding medium OCT™ and frozen at -80°C. Each portion was then cut into 5 µm sections on a cryostat and attached to glass slides. Finally, these samples were fixed with formaldehyde and incubated with DAPI (4,6-diamidino-2-phenylindole) for 15 min before the cover assembly. The presence of both fluorescently loaded nanoparticles in the intestinal mucosa and the cell nuclei stained with DAPI were visualized in a fluorescence microscope (Axioimager M1, Zeiss, Oberkochen, Germany) with a coupled

camera (Axiocam ICc3, Zeiss, Oberkochen, Germany) and fluorescent source (HBO 100, Zeiss, Oberkochen, Germany). The images were captured with the software ZEN (Zeiss, Oberkochen, Germany). As control, an aqueous suspension of Lumogen® F Red 305 was administered.

2.10. Protective study: sensitization, vaccination and challenge studies

Experiments were performed using a protocol previously described [36,37] and in compliance with the "Ethical and Biosafety Committee for Research on Animals" at the University of Navarra in line with the European legislation on animal experiments. CD-1 female mice of about 20 ± 1 grams were sensitized by orally administration of a mixture between of peanut butter (Capitan Mani® soft peanut butter; 4.35 mg with an approx. content of 1 mg protein) and 5 μg cholera toxin in a total volume of 200 μL of saline solution on days 1, 7, 15 and 21. Moreover a tape stripping was applied on the back of animals in order to obtain a higher sensitization. For this purpose, mice were shave and barrier-disrupted on back skin. Percutaneous sensitization in the damaged skin was performed by topical application of 100 μg peanut extract in 100 μL saline solution onto the barrier-disrupted skin.

On day 25, the sensitized animals were divided in 3 groups of ca. 15 animals each. Each group of animals received one of the following treatments: (i) saline (Control +), (ii) free peanut extract dispersed in water (PE), and (iii) PE-loaded nanoparticles (PE-GM-NP). In addition, a group of non-sensitized animals were also employed as control (Control-). On days 25, 28 and 35 the animals received one oral dose of 1 mg peanut extract either resuspended in purified water (PE) or incorporated into nanoparticles (PE-GM-NP).

Finally, on days 44 or 45 animals were challenged by an injection of 2 mg PE in 200 µL of saline solution by intraperitoneal route in order to provoke an anaphylactic shock in the sensitized animals. Figure 1S (Supplementary Material) summarizes the protocol.

In order to analyse the intensity of the anaphylaxis shock the following parameters were recorded: body temperature, mobility, bristly hair and cyanosis. Clinical anaphylactic reactions were scored by two independent observers. Piloerection and cyanosis were scored as follows: (−) absent (normal mouse), (+) weak reaction and/or scratching of the nose and head, (++) moderate, and (+++) strong. In a similar way, the mobility of animals was scored as very low (no reaction after pushing), low (arched back and low movements) or normal.

2.11. Statistical analysis

The physicochemical characteristics of nanoparticles as well as the in vitro studies were compared using the Student´s t test. For in vivo studies, comparisons were performed using the one-way analysis of the variance (ANOVA) and Tukey HSD test. In all cases $p<0.05$ was consider as a statistically significant difference. All calculations were performed using Graphpad Prism v6 (Graphpad Software, San Diego, CA).

3. Results

3.1. Synthesis and characterization of Gantrez-mannosamine conjugate (GM)

Gantrez-mannosamine conjugate was synthesised by the covalent binding of mannosamine to the anhydride groups of the copolymer of methylvinylether and maleic

anhydride (Gantrez® AN). Figure 2S (Supplementary Material) shows a schematic representation of this synthesis.

FTIR analysis, ^{1}H-NMR analysis (Figures 3S and 4S; Supplementary Material) and titration (Table 1S; Supplementary Material) were also performed. From these studies it was calculated that the synthesis produced a polymer conjugate in which about 20% of the carboxylic acid groups from hydrated poly(anhydride) would be used for the covalent binding of mannosamine. In other words, the percentage of substitution means that 20 molecules of the maleic anhydride groups of each 100 residues in Gantrez® AN had reacted with mannosamine to generate amide groups and carboxylic acids. From OPA analysis, the amount of mannosamine associated with the poly(anhydride) backbone was calculated to be about 21 μg/mg. Finally, with these data, the estimated MW of the conjugate (GM) was 97.54 kDa.

3.2. Preparation of mannosamine-modified nanoparticles

Nanoparticles were prepared from GM by a desolvation process using calcium as "bridge" between two neighbouring carboxylic acid residues of the polymer backbone (Figure 2S). Table 1 shows the main physico-chemical properties of these nanoparticles. PE-loaded nanoparticles (PE-GM-NP) displayed a slightly higher mean size (270 nm vs 190 nm) and a similar negative zeta potential (-33 vs. -37 mV) than unloaded ones (GM-NP). Interestingly, the preparative process employed here resulted in homogeneous batches of nanoparticles (PDI lower than 0.2). The PE loading was calculated to be 25 μg/mg nanoparticles with encapsulation efficiency of 80%. For fluorescently labelled nanoparticles, the amount of Lumogen® F Red 305 incorporated into the nanoparticles

was calculated to be similar for all the formulations tested and close to 7.3 µg/mg (data not shown).

The surface hydrophobicity of nanoparticles was evaluated by using the Rose Bengal test (data not shown). From these studies, the hydrophobicity of GM-NP was 30-times lower than for Gantrez nanoparticles (NP). However, after encapsulation of PE, the resulting nanoparticles (PE-GM-NP) displayed a 6-times higher hydrophobicity than empty ones (GM-NP).

The stability of nanoparticles was investigated by measuring the turbidity changes as a function of time in gastric (SGF) and intestinal (SIF) simulated fluids in a concentration of 3 mg/mL (Figure 1). Nanoparticles were easily dispersed in both media and no aggregation phenomenon were observed during the study. When incubated in SGF, both types of nanoparticles (loaded and empty) displayed a similar profile with a quite high stability for at least 1.5 h. In SIF, empty nanoparticles displayed a significantly higher stability than PE-loaded ones. Thus, for GM-NP, the turbidity of samples decreased during the first 30 min to reach a plateau of absorbance. At this moment, the turbidity of samples was about 70% of the initial values. For PE-GM-NP dispersed in SIF, the absorbance of samples decreased rapidly and after 90 min of incubation the absorbance was only of about 10% of the initial values.

3.3. *In vitro* release studies

Figure 2 shows the release profile of PE from GM nanoparticles as function of time when incubated in SGF (during the first 2 hours) and SIF (from 2 to 24 hours). In SGF only between 5-8% of the total payload of nanoparticles was released during the first 2 hours

of the experiment. In SIF, the release rate of PE from nanoparticles increased rapidly and, at the end of the experiment, all the PE content was released at the end of the experiment, as measured by ELISA.

3.4. *In vitro* evaluation of nanoparticles diffusion in mucus

Table 2 shows the diffusion coefficient in water (D°) calculated by the Stoke Einstein Equation, diffusion coefficient in the intestinal mucus <Deff> measured by the MPT technique and the ratio as percentage of these two parameters (Deff/D°) of the tested nanoparticles. This last parameter was employed to compare the diffusion of the nanoparticles in intestinal pig mucus after normalising the effect of particle size since D° is directly proportional to the particle size. GM-NP displayed a slightly higher diffusion coefficient than NP. For PE-loaded nanoparticles, the diffusion coefficient in the mucus was found to be about 12-fold higher than for unloaded nanoparticles prepared from the Gantrez-mannosamine (GM-NP). In all cases the relative efficiency of particles diffusion (Deff/D°) of these nanoparticles was higher than the diffusion of PLGA-NP control particles (0.0005 for PLGA-NP vs. 0.0190 and 0.2240 for GM-NP and PE-GM-NP respectively).

3.5. Gastrointestinal transit studies with ^{99m}Tc radiolabelled nanoparticles

Figure 3 shows the biodistribution (SPECT-CT images) of ^{99m}Tc-GM-NP orally administered to rats. One hour post-administration, an important fraction of the given dose of nanoparticles appeared to remain in the stomach of animals. Nanoparticles appeared to slowly enter in the small intestine and move along the gut over time. Likely,

at the end of the experiment, the no presence of radioactivity was observed in the liver or the lungs of the animals.

3.6. Biodistribution of nanoparticles orally administered

Figure 4 shows fluorescence microscopy images of ileum samples from animals treated with fluorescently labelled nanoparticles two hours post-administration. Empty nanoparticles (GM-NP) appeared to be mainly localized at the intestinal mucus layer (Figures 4A and 4B). On the other hand, PE-GM-NP displayed a higher capability for reaching the intestinal epithelium including the surface of Peyer´s patches (Figures 4C and 4D). As a control, an aqueous suspension of Lumogen was administered to rats (data not shown). In this case, Lumogen particles in gut were observed as long aggregates with no capacity to reach intestinal epithelium.

3.7. Protective study

Peanut sensitized animals received an immunotherapeutic schedule on days 4, 7, and 14 after sensitization. Then, on day 20, animals were challenged with the intraperitoneal administration of 2 mg peanut extract. In order to analyse the intensity of the anaphylaxis, several parameters were evaluated. Ten minutes after challenge, sensitized- and non -treated animals (Control +) experienced an important decrease of their body temperature. Animals treated either with free (PE) or encapsulated (PE-GM-NP) peanut extract displayed a significantly lower temperature variation ($p<0.05$).

Thirty minutes after challenge, mice were visually assessed for symptoms of anaphylaxis and assigned symptoms scores (Table 3). Animals from the non-treated group (Control

+) displayed a low mobility and strong signs of bristly hair and cyanosis, whereas animals treated with free PE present a slightly better symptomatology, in spite of their apparently lower body temperature than control animals. On the contrary, animals treated with peanut-loaded nanoparticles displayed a better symptomatology in terms of cyanosis and decrease of rectal temperature and even a slightly better ability to maintain some movements than animals from the other groups.

Figure 5 shows the cumulative survival of animals after the intraperitoneal administration of 2 mg PE. In the positive control group, 40 minutes after challenge, less than 10% of the animals were alive. On the other hand, for sensitized animals treated with PE, the survival rate was close to 30%, whereas for those animals treated with PE-GM-NP, this survival rate was 53%.

4. Discussion

The success of nanoparticle-based formulations as oral carriers for biologically active compounds (e.g., peptides or proteins) is highly dependent on their capabilities to both protect the cargo against its premature degradation under the harsh conditions of the gut, and reach the ideal site for its absorption and/or action. Particularly, nanoparticles for allergy immunotherapy should be able to induce, modulate and potentiate an adequate immune response in order to minimize the effect associated with an allergen exposure in susceptible individuals. In this context, recent studies have shown that the encapsulation of a roasted peanut extract in poly(anhydride) nanoparticles down-regulated the allergen-specific Th2 response, potentiating the specificTh1 response [26] and, therefore, offering protection in a murine model of peanut allergy [37].

In order to ameliorate these results, one possible strategy may be the use of functionalization of these poly(anhydride) nanoparticles with ligands capable of offering mucus-permeating properties and the ability of specifically binding receptors on the immune cells localized in the gut. In this context, nanoparticles were prepared from a polymer conjugate obtained by the covalent binding of mannosamine to the copolymer of methylvinylether and maleic anhydride (Gantrez® AN). The new resulting nanoparticles (GM-NP) displayed a mean size slightly higher than those obtained from Gantrez® AN (193 vs 178 nm). On the other hand, the zeta potential of both types of nanoparticles were negative and quite similar in an absolute value (-37 vs -43 mV). On the contrary, GM-NP displayed a 30-fold lower hydrophobic surface and a capability to diffuse in intestinal pig mucus of about 12-times higher than NP (Table 2). All of these evidences suggest that the hydrophilic residues of mannosamine would be mainly exposed on the surface of the nanoparticle. This idea is supported by previous works, where high diffusivity of particles was observed when they were coated with hydrophilic ligands [38,39]. In line with this, the low stability of mannosylated nanoparticles in SIF (Figure 1), with an important decrease of their initial size, would facilitate their capability to cross the mucus layer and reach the intestinal epithelium.

Regarding the in vitro properties of the peanut loaded nanoparticles, the release profile of PE from GM-NP was found to be dependent on the pH conditions (Figure 2). Thus, under simulated gastric conditions (pH 1.2), a small fraction (5-8%) of the loaded extract was released in two hours. On the contrary, under simulated intestinal conditions, the peanut content of nanoparticles was completely released in less than 24 hours of

incubation (Figure 2). Likely, this behaviour is in line with the stability study of these nanoparticles in SGF and SIF (Figure 1).

Furthermore, the encapsulation of PE increased the hydrophobicity of the resulting nanoparticles, evidencing the presence of components of this extract on the surface. Regarding the diffusion capabilities of nanoparticles in intestinal mucus, it was surprising to observe a significantly higher diffusivity for PE-loaded nanoparticles than for empty ones with a high hydrophilic character (Table 2). This result may be explained by a rapid release of peanut extract components located on the surface of the nanoparticles and their disturbing effects on the structural properties of the mucus gel. In fact, peanut proteins possess important emulsifying properties and oil binding capabilities [40] that may negatively affect to the viscoelastic properties of mucus [41]. These effects, as well as their resistance to enzymatic degradation, would facilitate the ability of some peanut proteins (e.g., Ara h2, Ara h6, Ara h7, oleosins) to cross the mucus barrier and the intestinal epithelium, before exposition to underlying immune cells [42-44].

Likely PE-GM-NP were able of reaching both the normal intestinal epithelium and the surface of Peyer's patches (Figure 4). These findings are in agreement with previous results showing strong interactions of mannosylated nanocarriers within the intestinal epithelium, including Peyer's patches [25,45].

Finally, the protective effect of PE-GM-NP therapy was evaluated in a model of pre-sensitized mice to peanut. For this purpose, the animals were intraperitoneally challenged with the peanut extract. Animals treated with the PE-GM-NP displayed both a lower decrease in their basal temperature and less severe symptomatology associated with anaphylactic shock, when compared with animals treated with PE or ascribed to

the positive control group (Table 3). In line with these results, animals treated with PE-GM-NP displayed a higher survival rate (53%) than animals treated with PE (35%) or the control group (6%) (Figure 5). In spite of the important differences, no statistical differences from the cumulative survival rate or mice treated with either PE or PE-GM-NP was found. This lack of differences would be related to the limitations of our study, mainly associate with the number of animals involved in the study. Nevertheless, and based on the obtained results, the promising protective effect of PE-GM-NP observed in this study should be confirmed in a larger study involving a higher number of animals.

In conclusion, nanoparticles based in a new Gantrez-mannosamine conjugate may be easily prepared by a desolvation procedure followed by a cross-linking process with calcium ions. These nanoparticles may be employed to load and carry a peanut extract, facilitating their biodistribution within the gut, including Peyer's Patches. In addition, this nanoparticle-based formulation offers an important protection against the effects induced by an anaphylactic shock in peanut sensitized animals. However, further studies are needed in order to corroborate the promising protection offered by PE-GM-NP in an experimental model of peanut allergy.

Acknowledgments

The research leading to these results has received funding from the European Community's Seventh Framework Programm [FP7/2007-2013] for ALEXANDER under grant agreement nº NMP-2011-1.2-2-28076. Ana Brotons-Canto acknowledges the "Asociación de Amigos Universidad de Navarra" for the financial support.

Conflicts of Interest

The authors declare no conflict of interest.

References

1. Lomas JM, Järvinen KM. Managing nut-induced anaphylaxis: challenges and solutions. *J Asthma Allergy*. 2015;8:115-123. doi:10.2147/JAA.S89121
2. Boden SR, Wesley Burks A. Anaphylaxis: a history with emphasis on food allergy. *Immunol Rev*. 2011;242(1):247-257. doi:10.1111/j.1600-065X.2011.01028.x
3. Patel N, Herbert L, Green TD. The emotional, social, and financial burden of food allergies on children and their families. *Allergy Asthma Proc*. 2017;38(2):88-91. doi:10.2500/aap.2017.38.4028
4. Walkner M, Warren C, Gupta RS. Quality of life in food allergy patients and their families. *Pediatr Clin North Am*. 2015;62(6):1453-1461. doi:10.1016/j.pcl.2015.07.003
5. Avery NJ, King RM, Knight S, Hourihane JO. Assessment of quality of life in children with peanut allergy. *Pediatr Allergy Immunol*. 2003;14(5):378-382.
6. Gernez Y, Nowak-Węgrzyn A. Immunotherapy for food allergy: are we there yet? *J Allergy Clin Immunol Pract*. 2017;5(2):250-272. doi:10.1016/j.jaip.2016.12.004
7. Vickery BP, Lin J, Kulis M, Fu Z, Steele PH, Jones SM, Scurlock AM, Gimenez G, Bardina L, Sampson HA, Burks AW. Peanut oral immunotherapy modifies IgE and IgG4 responses to major peanut allergens. *J Allergy Clin Immunol*. 2014;131(1):128-134. doi:10.1016/j.jaci.2012.10.048.

8. Burton OT, Logsdon SL, Zhou JS, Medina-Tamayo J, Abdel-Gadir A, Noval Rivas M, Koleoglou KJ, Chatila TA, Schneider LC, Rachid R, Umetsu DT, Oettgen HC. Oral immunotherapy induces IgG antibodies that act via FcγRIIb to suppress IgE-mediated hypersensitivity. *J Allergy Clin Immunol*. 2014;134(6):1310-1317. doi: 10.1016/j.jaci.2014.05.042.

9. Wang J, Sampson HA. Oral and sublingual immunotherapy for food allergy. *Asian Pac J Allergy Immunol*. 2013;31(3):198-209.

10. Hofmann AM, Scurlock AM, Jones SM, et al. Safety of a peanut oral immunotherapy protocol in children with peanut allergy. *J Allergy Clin Immunol*. 2009;124(2):286-291.e6. doi:10.1016/j.jaci.2009.03.045

11. Umetsu DT, Rachid R, Schneider LC. Oral immunotherapy and anti-IgE antibody treatment for food allergy. *WAO J*. 2015;8(1):20. doi:10.1186/s40413-015-0070-3

12. De Souza Rebouças J, Esparza I, Ferrer M, Sanz ML, Irache JM, Gamazo C. Nanoparticulate adjuvants and delivery systems for allergen immunotherapy. *J Biomed Biotechnol*. 2012;2012:13,474605. doi:10.1155/2012/474605

13. Gamboa JM, Leong KW. In vitro and in vivo models for the study of oral delivery of nanoparticles. *Adv Drug Deliv Rev*. 2013;65(6):800-810. doi:10.1016/j.addr.2013.01.003

14. Bohle B, Jahn-Schmid B, Maurer D, Kraft D, Ebner C. Oligodeoxynucleotides containing CpG motifs induce IL-12, IL-18 and IFN-? production in cells from allergic individuals and inhibit IgE synthesis in vitro. *Eur J Immunol*. 1999;29(7):2344-2353.

15. Hayen SM, Kostadinova AI, Garssen J, Otten HG, Willemsen LEM. Novel immunotherapy approaches to food allergy. *Curr Opin Allergy Clin Immunol*. 2014;14(6):549-556. doi:10.1097/ACI.0000000000000109

16. Gregory AE, Titball R, Williamson D. Vaccine delivery using nanoparticles. *Front Cell Infect Microbiol*. 2013;3:13. doi: 10.3389/fcimb.2013.00013

17. Gamazo C, Gastaminza G, Ferrer M, Sanz ML, Irache JM. Nanoparticle based-immunotherapy against allergy. *Immunotherapy*. 2014;6(7):885-897. doi:10.2217/imt.14.63

18. Peterson WL, Artis D. Intestinal epithelial cells: regulators of barrier function and immune homeostasis. *Nat Rev Immunol*. 2014;14(3):141-153. doi: 10.1038/nri3608

19. Ensign LM, Cone R, Hanes J. Oral drug delivery with polymeric nanoparticles: the gastrointestinal mucus barriers. *Adv Drug Deliv Rev*. 2012;64(6):557-570. doi:10.1016/j.addr.2011.12.009

20. Cone RA. Barrier properties of mucus. *Adv Drug Deliv Rev*. 2009;61(2):75-85. doi:http://dx.doi.org/10.1016/j.addr.2008.09.008

21. Boddupalli BM, Mohammed ZNK, Nath RA, Banji D. Mucoadhesive drug delivery system: An overview. *J Adv Pharm Technol Res*. 2010;1(4):381-387. doi:10.4103/0110-5558.76436

22. Inchaurraga L, Martín-Arbella N, Zabaleta V, Quincoces G, Peñuelas I, Irache JM. In vivo study of the mucus-permeating properties of PEG-coated nanoparticles following oral administration. *Eur J Pharm Biopharm*. 2015;97(Pt A):280-289. doi:10.1016/j.ejpb.2014.12.021

23. Netsomboon K, Bernkop-Schnürch A. Mucoadhesive vs. mucopenetrating particulate drug delivery. *Eur J Pharm Biopharm*. 2016;98:76-89. doi:10.1016/j.ejpb.2015.11.003

24. Salman HH, Irache JM, Gamazo C. Immunoadjuvant capacity of flagellin and mannosamine-coated poly(anhydride) nanoparticles in oral vaccination. *Vaccine*. 2009;27(35):4784-4790. doi:10.1016/j.vaccine.2009.05.091

25. Salman HH, Gamazo C, Campanero MA, Irache JM. Bioadhesive mannosylated nanoparticles for oral drug delivery. *J Nanosci Nanotechnol*. 2006;6(9-10):3203-3209.

26. De S. Rebouças J, Irache JM, Camacho AI, Gastaminza G, Sanz ML, Ferrer M, Gamazo C. Immunogenicity of peanut proteins containing poly(anhydride) nanoparticles. *Clin Vaccine Immunol*. 2014;21(8):1106-1112. doi:10.1128/CVI.00359-14

27. Tamayo I, Irache JM, Mansilla C, Ochoa-Repáraz J, Lasarte JJ, Gamazo C. Poly(anhydride) nanoparticles act as active Th1 adjuvants through toll-like receptor exploitation. *Clin Vaccine Immunol*. 2010;17(9):1356-1362. doi:10.1128/CVI.00164-10

28. Royer PJ, Emara M, Yang C, Al-Ghouleh A, Tighe P, Jones N, Sewell HF, Shakib F, Martinez-Pomares L, Ghaemmaghami AM. The mannose receptor mediates the uptake of diverse native allergens by dendritic cells and determines allergen-induced T cell polarization through modulation of IDO activity. *J Immunol*. 2010;185(3):1522-1531. doi:10.4049/jimmunol.1000774

29. Ando T, Hatsushika K, Wako M, et al. Orally administered TGF-β is biologically

active in the intestinal mucosa and enhances oral tolerance. *J Allergy Clin Immunol*. 2007;120(4):916-923. doi:10.1016/j.jaci.2007.05.023

30. Benson JR, Hare PE. O-phthalaldehyde: fluorogenic detection of primary amines in the picomole range. Comparison with fluorescamine and ninhydrin. *Proc Natl Acad Sci*. 1975;72(2):619-622. doi:10.1073/pnas.72.2.619

31. Arbos P, Wirth M, Arangoa MA, Gabor F, Irache JM. Gantrez AN as a new polymer for the preparation of ligand-nanoparticle conjugates. *J Control Release*. 2002;83(3):321-330.

32. Doktorovova S, Shegokar R, Martins-Lopes P, Silva AM, Lopes CM, Müller RH, Souto EB. Modified Rose Bengal assay for surface hydrophobicity evaluation of cationic solid lipid nanoparticles (cSLN). *Eur J Pharm Sci*. 2012;45(5):606-612. doi:10.1016/j.ejps.2011.12.016

33. Abdulkarim M, Agulló N, Cattoz B, Griffiths P, Bernkop-Schnürch A, Borros SG, Gumbleton M. Nanoparticle diffusion within intestinal mucus: Three-dimensional response analysis dissecting the impact of particle surface charge, size and heterogeneity across polyelectrolyte, pegylated and viral particles. *Eur J Pharm Biopharm*. 2015;97(Pt A):230-238. doi:10.1016/j.ejpb.2015.01.023

34. Grießinger J, Dünnhaupt S, Cattoz B, Griffiths P, Oh S, Borrós i Gómez S, Wilcox M, Pearson J, Gumbleton M, Abdulkarim M, Pereira de Sousa I, Bernkop-Schnürch A. Methods to determine the interactions of micro- and nanoparticles with mucus. *Eur J Pharm Biopharm*. 2015;96:464-476. doi:10.1016/j.ejpb.2015.01.005

35. Areses P, Agüeros MT, Quincoces G, Collantes M, Richter JÁ, López-Sánchez LM, Sánchez-Martínez M, Irache JM, Peñuelas I. Molecular imaging techniques to

study the biodistribution of orally administered 99mTc-labelled naive and ligand-tagged nanoparticles. *Mol Imaging Biol*. 2011;13(6):1215-1223. doi:10.1007/s11307-010-0456-0

36. Gamazo C, García-Azpíroz M, De S. Rebouças J, Gastaminza G, Ferrer M, Irache JM. Oral immunotherapy using polymeric nanoparticles loaded with peanut proteins in a murine model of fatal anaphylaxis. *Immunotherapy*. 2017;9(15):1205-1217. doi:10.2217/imt-2017-0111

37. Brotons-Canto A, Gamazo C, Martín-Arbella N, Abdulkarim M, Matías J, Gumbleton M, Irache JM. Evaluation of nanoparticles as oral vehicles for immunotherapy against experimental peanut allergy. *Int J Biol Macromol*. 2018;110:328-335. doi:10.1016/j.ijbiomac.2017.09.109

38. Tariq M, Alam MA, Singh AT, Panda AK, Talegaonkar S. Surface decorated nanoparticles as surrogate carriers for improved transport and absorption of epirubicin across the gastrointestinal tract: Pharmacokinetic and pharmacodynamic investigations. *Int J Pharm*. 2016;501(1-2):18-31. doi:10.1016/j.ijpharm.2016.01.054

39. Pereira De Sousa I, Moser T, Steiner C, Fichtl B, Bernkop-Schnürch A. Insulin loaded mucus permeating nanoparticles: Addressing the surface characteristics as feature to improve mucus permeation. *Int J Pharm*. 2016;500(1-2):236-244. doi:10.1016/j.ijpharm.2016.01.022

40. Jain A, Prakash M, Radha C. Extraction and evaluation of functional properties of groundnut protein concentrate. *J Food Sci Technol*. 2015;52(10):6655-6662. doi:10.1007/s13197-015-1758-7

41. Lock JY, Carlson TL, Wang CM, Chen A, Carrier RL. Acute Exposure to Commonly Ingested Emulsifiers Alters Intestinal Mucus Structure and Transport Properties. *Sci Rep*. 2018;8(1):1-14. doi:10.1038/s41598-018-27957-2

42. Chambers SJ, Wickham MSJ, Regoli M, Bertelli E, Gunning PA, Nicoletti C. Rapid in vivo transport of proteins from digested allergen across pre-sensitized gut. *Biochem Biophys Res Commun*. 2004;325(4):1258-1263. doi:10.1016/j.bbrc.2004.10.161

43. Moreno FJ, Clemente A. 2S Albumin storage proteins: what makes them food allergens? *Open Biochem J*. 2008;2:16-28. doi:10.2174/1874091X00802010016

44. Price D, Ackland L, Suphioglu C. Nuts and guts transport of food allergen across the intestinal ephitelium. *Asia Pac Allergy*. 2013;3:257-265.

45. Xu B, Zhang W, Chen Y, Xu Y, Wang B, Zong L. Eudragit® L100-coated mannosylated chitosan nanoparticles for oral protein vaccine delivery. *Int J Biol Macromol*. 2018;113:534-542. doi:10.1016/j.ijbiomac.2018.02.016

Figure captions

Figure 1. Stability of empty (GM-NP) or peanut loaded nanoparticles (PE-GM-NP) in simulated gastric fluid (SGF, pH 1.2) or in simulated intestinal fluid (SIF, pH 6.8). Data expressed as mean ± SD (n=3).

Figure 2. In vitro release of peanut extract from PE-GM-NP. Data expressed as cumulative amount of PE released versus time. Data expressed as mean ± SD (n=3).

Figure 3. Volume rendered fused SPECT-CT images from representative rats at 1, 2 and 4 hours after administration of ^{99m}Tc-labelled GM-NP by oral gavage.

Figure 4. Fluorescent microscopic visualization of lumogen red-loaded nanoparticles (GM and PE-GM-NP) in longitudinal sections of the ileum of rats. Figures A and B correspond to empty formulations (GM-NP) whereas C and D refer to peanut-loaded nanoparticles (PE-GM-NP). The draw in the middle indicates the anatomical regions for the mucosal intestinal villi (M), the follicle-associated epithelium of Peyer`s Patches (PP), and Lumen (L). Arrows in figures indicate the intestinal portions with high interaction between nanoparticles and mucosal intestinal villi. DAPI staining of nuclei appears as blue.

Figure 5. Cumulative survival rate of mice intraperitoneally challenge with peanut. Animals were treated with a peanut extract administered either free (PE) or encapsulated into nanoparticles (PE-GM-NP). Sensitized untreated animals (Control +)

and non-sensitized mice (Control -) were also included. (**p< 0.01, Log rank test indicates significant differences between animals treated with PE-GM-NP and non-treated animals. Log rank test indicate significant differences between free peanut extract and non-treated animals *($p < 0.05$).

Table 1. Physico-chemical characteristics of empty (GM-NP) and peanut loaded nanoparticles (PE-GM-NP). PDI: polydispersity index; PE: peanut extract; EE: encapsulation efficacy. Data expressed as mean ± SD (n=3).

Formulation	**Mean size (nm)**	**PDI**	**Zeta potential (mV)**	**Yield (%)**	**PE loading (µg/mg)**	**EE (%)**
GM-NP	193 ± 3	0.15 ± 0.01	-37 ± 4	87	-	-
PE-GM-NP	274 ± 2	0.16 ± 0.01	-33 ± 4	67	25 ± 2	81 ± 6

Table 2. Nanoparticle diffusion kinetics in intestinal pig mucus. Data expressed as mean ± SD (n=3). D°: diffusion coefficient in water; <Deff>: diffusion coefficient in mucus; %<Deff>/ D° ratio: relative efficiency of particles diffusion; R: ratio of %<Deff>/ D° of the formulations tested. PLGA-NP: PLGA nanoparticles; GM-NP: empty nanoparticles; PE-GM-NP: PE-loaded nanoparticles.

	D° (water) $cm^2 \times S^{-1} \times 10^{-9}$	**<Deff> (mucus) $cm^2 \times S^{-1} \times 10^{-9}$**	**%<Deff>/ D° ratio**	**R**
PLGA-NP	27.91	0.0001 (± 0.0002)	0.0005	0.03
NP	25.69	0.0004 (± 0.0003)	0.0016	0.084
GM-NP	18.57	0.0035 (± 0.0018)	0.0190	1.00
PE-GM-NP	23.79	0.0531 (± 0.0313)	0.2240	11.79

Table 3. Anaphylactic symptoms after allergic provocation challenge in peanut-sensitized CD-1 mice. Animals were treated with a peanut extract administered either free (PE) or encapsulated into nanoparticles (PE-GM-NP). Sensitized untreated animals (Control +) and non-sensitized mice (Control -) were also included.

Treatment	**ΔTemperature (ºC)**	**Piloerection**	**Mobility**	**Cyanosis**
Control +	-4.7 ± 2.6	+++	Very low	+++
PE	-5.2 ± 3.2	++	Very low	++
PE-GM-NP	-3.6 ± 2.7	++	Low	+
Control -	0.5 ± 0.8	-	Normal	-

Severity of the symptoms: (-) absent, (+) weak, (++) moderate, (+++) strong

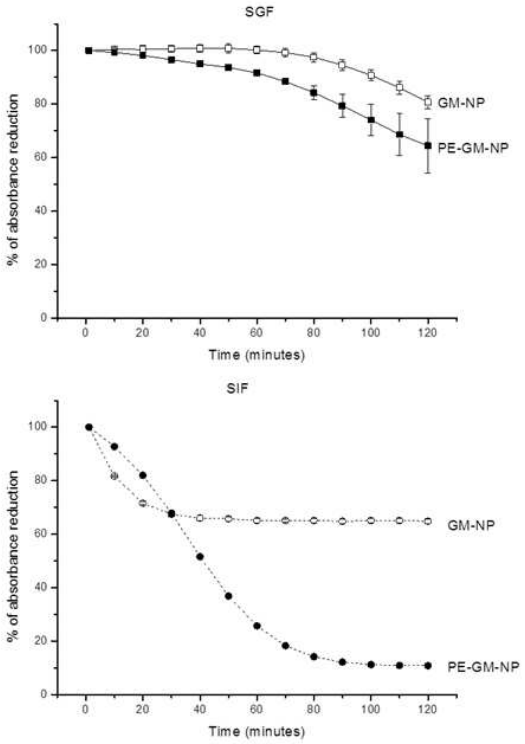
SGF
% of absorbance reduction
Time (minutes)
GM-NP
PE-GM-NP
SIF
% of absorbance reduction
Time (minutes)
GM-NP
PE-GM-NP

Figure 1

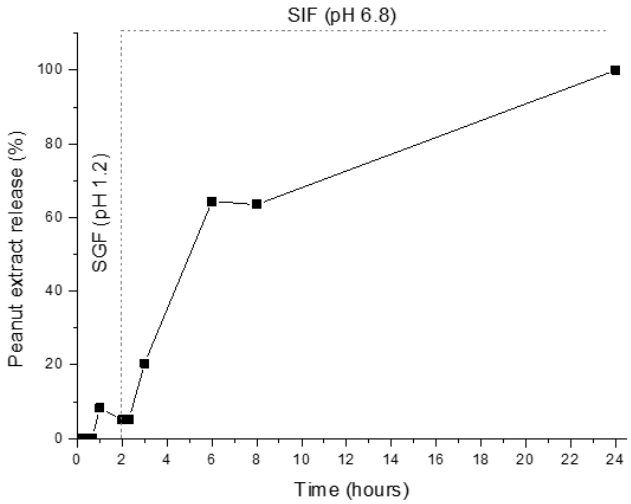
SIF (pH 6.8)
SGF (pH 1.2)
Peanut extract release (%)
Time (hours)
0
20
40
60
80
100
0
2
4
6
8
10
12
14
16
18
20
22
24

Figure 2

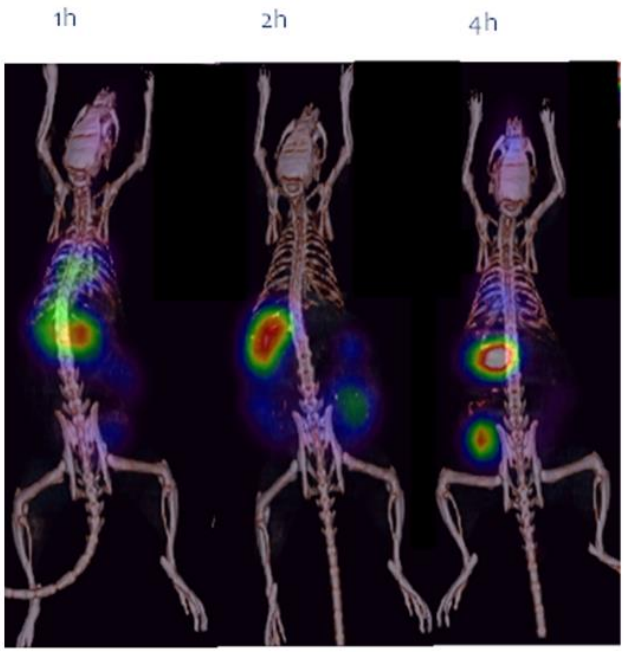

Figure 3

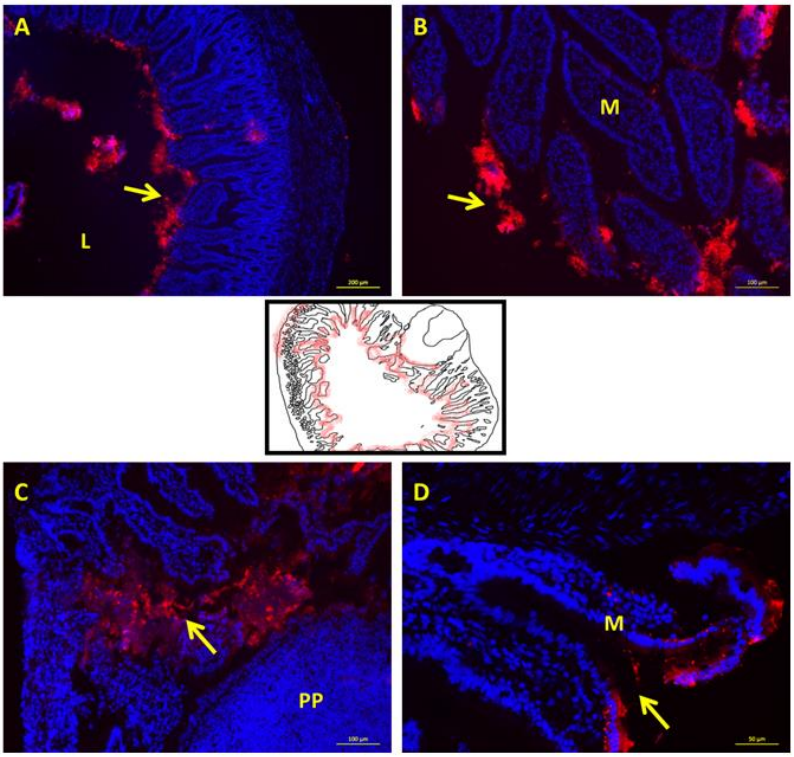

Figure 4

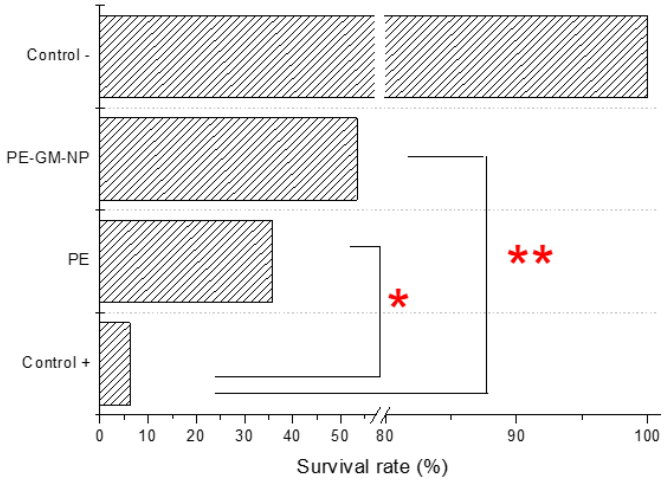
Control -
PE-GM-NP
PE
Control +
*
**
0
10
20
30
40
50
80
90
100
Survival rate (%)

Figure 5

Supplementary Material

Mannosylated nanoparticles for oral immunotherapy in a murine model of peanut allergy

Ana Brotons-Canto, Carlos Gamazo, Nekane Martín-Arbella, Muthanna Abdulkarim, Mark Gumbleton, Gemma Quincoces, Ivan Peñuelas, Juan M. Irache

Methods

Characterization of Gantrez® AN-mannosamine conjugates

The covalent insertion of mannosamine in the polymer chain was confirmed by infrared spectroscopy, elemental analysis, ^{1}H-NMR and titration. The amount of mannosamine bound to the poly(anhydride) was estimated by the OPA method [1].

IR analysis

The binding between the poly(anhydride) and mannosamine was evaluated by Fourier transform infrared spectroscopy (FTIR). Spectra were collected in a Nicolet-FTIR Avatar 360 spectrometer (Thermo/Nicolet 360 FT IR E.S.P., Thermo Fisher Scientific, Waltham, Massachusetts, USA), using a MKII Golden Gate ATR device with resolution of 2 cm-1 connected with OMNIC E.S.P. software (Thermo Fisher Scientific, Waltham, Massachusetts, USA). The spectrum obtained was an average of 32 scans.

Elemental analysis

The C, H, O and N contents of the synthesized conjugates were determined in a LECO CHN-900 apparatus (Michigan, USA). For this purpose, 1 mg of each polymer was analysed by triplicate and the results were expressed as percentage (% w/w).

^{1}H-NMR

NMR spectra were obtained in a Bruker UltraShield NMR (400 MHz/54 mmA) Avance 400 (Switzerland). For this purpose, an exactly weighed amount of samples were dissolved in deuterated DMSO and the spectra were obtained at ns = 6400.

Titration

The poly(anhydride) and its conjugate were first hydrated and dispersed in water till their total solubilisation. At this moment, the aqueous solutions of the polymers were titrated with NaOH 0.2N in the presence of phenolphthalein as indicator. Titration was used to measure the percentage of free carboxylic groups and to calculate the degree of substitution (DS) of the resulting conjugate. The decrease of the carboxylic groups in the polymer conjugates in comparison to unmodified Gantrez® AN evidenced the ligand binding.

Mannosamine quantification

The amount of mannosamine covalently attached to the poly(anhydride) was indirectly quantified by the O-phthalaldehyde (OPA) assay for primary amines. For this purpose, 100 mg of unpurified GM were dissolved in 5 mL of acetone. Then, nanoparticles were obtained by the addition of 10 mL of a hydroalcoholic mixture (2.5 mL water and 7.5 mL Ethanol) containing 20 mL calcium chloride (0.8% w/v). The organic solvents were eliminated by evaporation under reduced pressure (Büchi R-144, Switzerland) and the resulting nanosuspension was centrifuged for 20 min at 40,000 x g (Sigma 3K30 Rot.,

12150-H, UK). Supernatants were collected for quantification of the mannosamine content.

The amount of mannosamine bound to the polymer backbone was estimated by difference between the initial amount of mannosamine added for the preparation of the conjugate and the amount of primary amines quantified in the supernatants.

Physico-chemical characterization of nanoparticles

Size, polydispersity index (PDI) and zeta potential

The mean size and the zeta potential of nanoparticles were determined by photon correlation spectroscopy (PCS) and electrophoretic laser Doppler anemometry, respectively, using a Zetaplus apparatus (Brookhaven Instruments Corporation, Holtsville, USA). The diameter of the nanoparticles was determined after dispersion in ultrapure water (1/10) and measured at 25 ºC by dynamic light scattering angle of 90 ºC. The zeta potential was determined as follows: 200 µL of the samples were diluted in 2 mL of a 0.1 mM KCl solution adjusted to pH 7.4. The yield of the preparative process of nanoparticles was calculated by gravimetry [2].

Surface hydrophobicity evaluation

The surface hydrophobicity of unloaded and loaded nanoparticles was evaluated by the Rose Bengal test as previously described [3], with some modifications. Briefly, 200 µL of nanoparticle suspensions, with increasing concentrations of nanoparticles (from 0.03 to 3 mg/mL), were mixed with 400 µL of a Rose Bengal aqueous solution (100 µg/mL). All samples were incubated under constant shaking at 1500 rpm, for 30 min at 25 ºC (Labnet VorTemp 56 EVC, Labnet International, Inc.). Afterwards, the samples were centrifuged at 13,500 x g for 30 min (centrifuge MIKRO 220, Hettich, Germany). The quantity of free RB in dispersion was determined by interpolation from a calibration curve. The concentration of RB bound to the nanoparticle surface was calculated as the difference between total concentration of RB used in the assay and free RB. Then, the hydrophobicity was calculated as the slope of the plot of partitioning quotient (PQ) vs. total surface area (TSA).

Quantification of the peanut extract loaded in nanoparticles

The amount of peanut encapsulated into nanoparticles was measured by using the bicinchonic acid method (microBCA). Briefly, 10 mg nanoparticles were resuspended in 1 mL water and centrifuged at 40,000 x g (Sigma 3K30 Rot. 12150-H, UK) for 20 min. Then, the precipitate was dissolved in 1 mL NaOH 0.1N and kept for 1 h at 37 ºC with constant agitation. Samples were assay in triplicate and results of PE loading were expressed as the amount of PE (in µg) per mg nanoparticles whereas the entrapment efficiency (EE, expressed in %) was determined by relating the estimated total weight of proteins entrapped in the batch of nanoparticles to the initial weight of proteins initially added.

Stability of nanoparticles in vitro

The stability of nanoparticles was evaluated by measuring the turbidity changes as a function of time in buffer solutions with different pH value corresponded to simulated gastric and intestinal fluids (see below) SGF and SIF (i.e., pH 1.2 and 6.8, respectively). This analysis was performed on unloaded and loaded nanoparticles for more than 2 hours in the SGF and SIF fluids.

Briefly, nanoparticles were firstly dispersed in purified water (6 mg/mL). Then, each suspension was mixed with a similar volume of either simulated gastric or intestinal fluid (1:1 v/v). The turbidity changes were monitored in a spectrophotometer at 405 nm in continuous kinetic measurements during 2 h (Labsystems EMS Reader MF). All measurements were performed by triplicate, and the results were expressed as percentage of absorbance reductions vs. time.

In vitro evaluation of nanoparticles diffusion in mucus

The diffusion of nanoparticles through porcine intestinal mucus barrier, as an in vitro measurement of their mucus-permeating properties, was assessed by Multiple Particle Tracking (MPT) technique. Mucus was isolated and standardized following the procedure described previously by Peason and coworkers [4,5]. For this purpose, pig small intestines were obtained from a local abattoir immediately after slaughter and transported on ice to the laboratory. Sections of the intestines that did not visibly contain chyme were cut into 15 cm lengths and mucus was removed. To remove the mucus gentle pressure was applied to one end of the length with the fingers and continuously applied unidirectionally to the opposite end. Samples (0.5 g) of porcine intestinal mucus were incubated in glass-bottom MatTek imaging dishes at 37°C. The fluorescently labelled nanoparticles were inoculated into each 0.5 g mucus sample in a 25 µL aliquot at a suspension concentration of 0.002% formulation. Each sample was incubated for 2 hours prior to video microscopy, in order to ensure effective particle distribution after inoculation. Video capture involved 2-dimensional imaging on a Leica DM IRB wide-field epifluorescence microscope (x63 magnification oil immersion lens) using a high speed camera (Allied Vision Technologies, UK) capturing 30 frames/second during 10 seconds (i.e. completed video film comprised 300 frames). For each 0.5 g mucus sample, a minimum of 300 individual trajectories were tracked and analysed.

Videos were imported into Fiji ImageJ software to convert the movement of each nanoparticle into individual trajectories across the full duration of the 10 s videos. However, for the analysis of particle diffusion only a 30 frame video period (1 s) was used, with the criterion that any individual particle tracked must display a continuous presence in the X–Y plane throughout the respective 30 sequential frames. Limiting the period of analysis to 30 frames minimized the impact of mucin movement upon the particle diffusion calculations. The individual particle trajectories were converted into numeric pixel data (Mosaic Particle Tracker within Fiji ImageJ) which, based on the microscope and video capture settings, were converted into metric distance. The distances moved by every individual particle over time in the X–Y trajectory were then expressed as a squared displacement (SD). The mean square displacement (MSD) of any single particle represents the geometric mean of that particle's squared displacements throughout its entire 30-frame trajectory. MSD was determined as follows:

$$\mathrm{MSD} = \left(\mathrm{X}_{\Delta \mathrm{t}}\right)^2 + \left(\mathrm{Y}_{\Delta \mathrm{t}}\right)^2$$

In any single mucus sample experiment an MSD was calculated for at least each of 100 individual particles (i.e., 100 MSD calculations) with the experiment replicated a further two times for any particle type. The Effective Diffusion Coefficient (D_{eff}) for a particular nanoparticle type was then calculated by:

$$Deff = \frac{MSD}{4 * \Delta t}$$

where 4 is a constant relating to the 2-dimensional mode of video capture and Δt is the selected time interval.

In order to compare the diffusion of nanoparticles after accounting the nanoparticles size the diffusion of all particles was also expressed as the parameter, % ratio $[D_{eff}]/[D°]$. So that, diffusion coefficient (D°) in water was calculated by the Stokes–Einstein equation at a temperature of 37°C:

$$D° = \frac{\kappa T}{6\pi \eta r}$$

In which κ is the Boltzmann constant, T is absolute temperature, η is water viscosity and r is radius of the particle.

Radiolabelling of nanoparticles

Briefly, 1–2 mCi of freshly eluted 99mTc-pertechnetate was reduced with 0.03 mg/mL stannous chloride and the pH was adjusted to 4 with 0.1 N HCl. Then, 2 mg nanoparticles in 1 mL water and 99mTc were added to pre-reduced tin. The mixture was vortexed for 30 s and incubated at room temperature for 10 min. The overall procedure was carried out in helium-purged vials.

The radiochemical purity was examined by paper chromatography (Whatman 3MM) developed with NaCl 0.9%. The labelling yield was always over 90%. Then, the gastro-intestinal fate of these radiolabelled nanoparticles was studied in male Wistar rats weighing 250-300 g that had fasted for 12 h.

Protective study: sensitization, vaccination and challenge studies

Figure 1S shows a schematic representation of the in vivo protective study.

Figure 1S. Experimental protocol of the protective study. CD-1 mice were sensitized intragastrically (i.g) with peanut extract together with cholera toxin for 4 weeks. Then animals received the treatments (corresponding to 1 mg PE each) on days 25, 28 and 35. Peanut hypersensitive mice were treated i.g. with either free peanut extract (n=14) or encapsulated in PE-GM-NP (n=15) 1 mg/mouse/day in 0.4 mL water. In addition, a group of peanut allergic mice received only saline (control +, n= 16) and a group of non-sensitized animals (control –, n=3) were monitored.

Results

Synthesis and characterization of Gantrez-mannosamine conjugate (GM)

GM was synthesised by the covalent binding of mannosamine to the anhydride groups of the copolymer of methylvinylether and maleic anhydride (Gantrez® AN) (Figure 2S). The figure also shows the effect of calcium as linker for the preparation of nanoparticles.

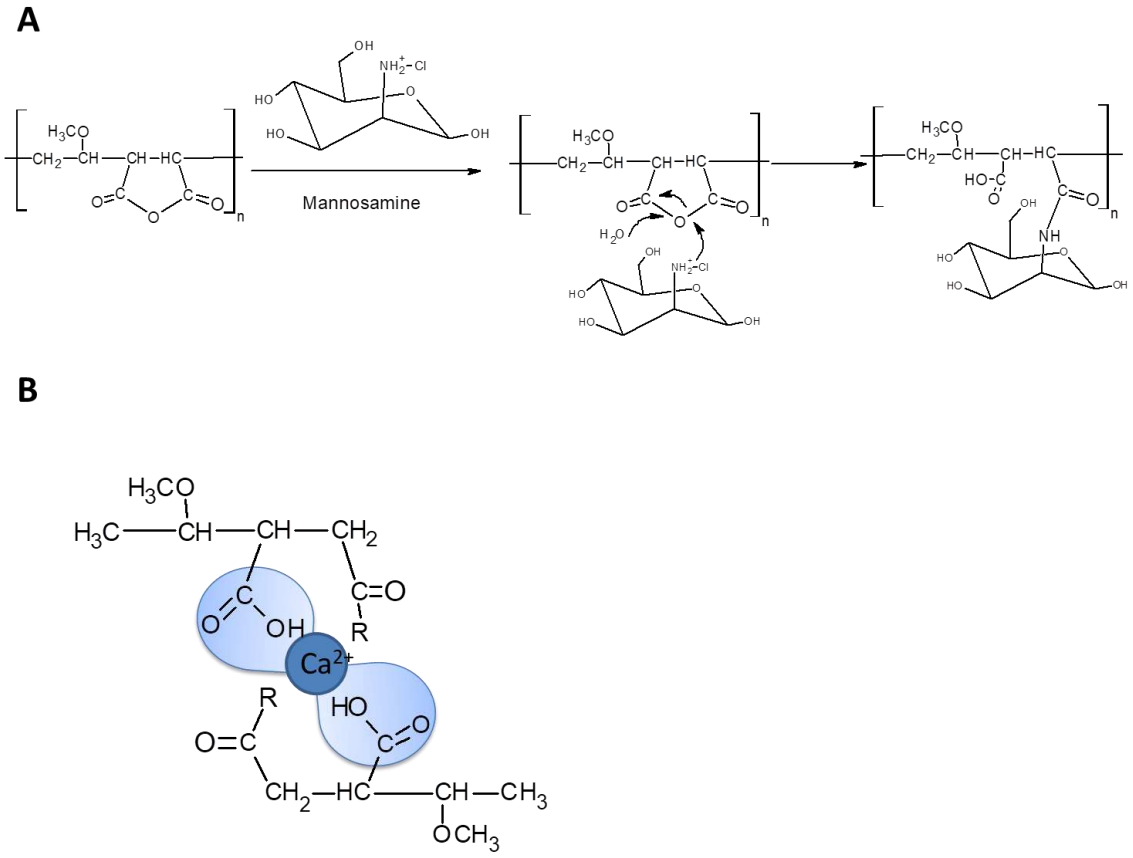

Figure 2S. Schematic representation of the reaction between mannosamine and Gantrez® AN (A), and the effect of calcium used for the preparation of nanoparticles (B). R represents mannosamine.

For the characterization of GM, FTIR analysis was performed to confirm the binding of the reactive functional groups of mannosamine (-OH or –NH2) to the anhydride groups of the polymer. Figure 3S shows the IR spectra for Gantrez® AN and GM. Both compounds presented bands at 1770-1850 cm^{-1} (Figure 3S, number 1), that are associated with a typical υ(C=O) signal characteristic of anhydride groups. For GM, the IR spectra showed an additional peak at 1707 cm^{-1} (Figure 3S, number 2), corresponding to an amide group. This signal confirmed that mannosamine was bound to the Gantrez through the amine functional group (Figure 3S, number 3). This binding was also evidenced by elemental analysis (Table 1S). Thus, the binding of mannosamine to the polymer backbone slightly decreased the percentage of carbon, whereas the hydrogen

and oxygen content increased. In the same way, a very low amount of nitrogen was detected in GM samples (Table 1S). Finally, Figure 4S shows the ^{1}H-NMR analysis of GM.

Table 1S. Physico-chemical characterization of Gantrez® AN (G) and its conjugate with mannosamine (GM). For titration and OPA experiments, data expressed as mean ± SD (n=3). M: mannosamine.

	C%	H%	O%	N%	% Free -COOH	DS (%)	MW (kDa)	Ligand content (µg M/mg)
G	53.49	5.18	41.33	0	100	0	95.50	-
GM	52.84	5.40	41.73	0.03	80.0 ± 0.7	20	97.54	20.90±0.84

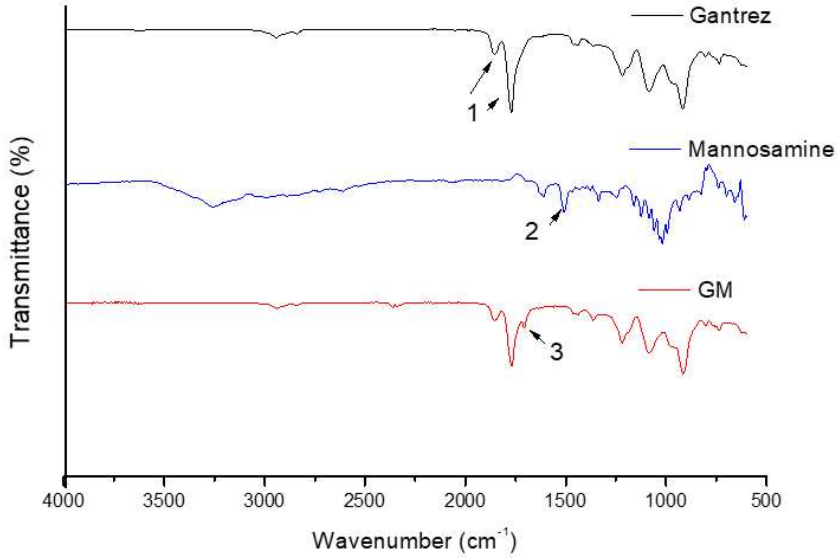

Figure 3S. IR spectra of Gantrez® AN polymer, mannosamine, and Gantrez® AN-mannosamine conjugate. Number 1 shows the typical bands of the anhydride groups. Number 2 illustrates the band corresponding to C-N stretching. Number 3 shows the amide group formed by the binding of mannosamine to the poly(anhydride) chain.

a) Gantrez

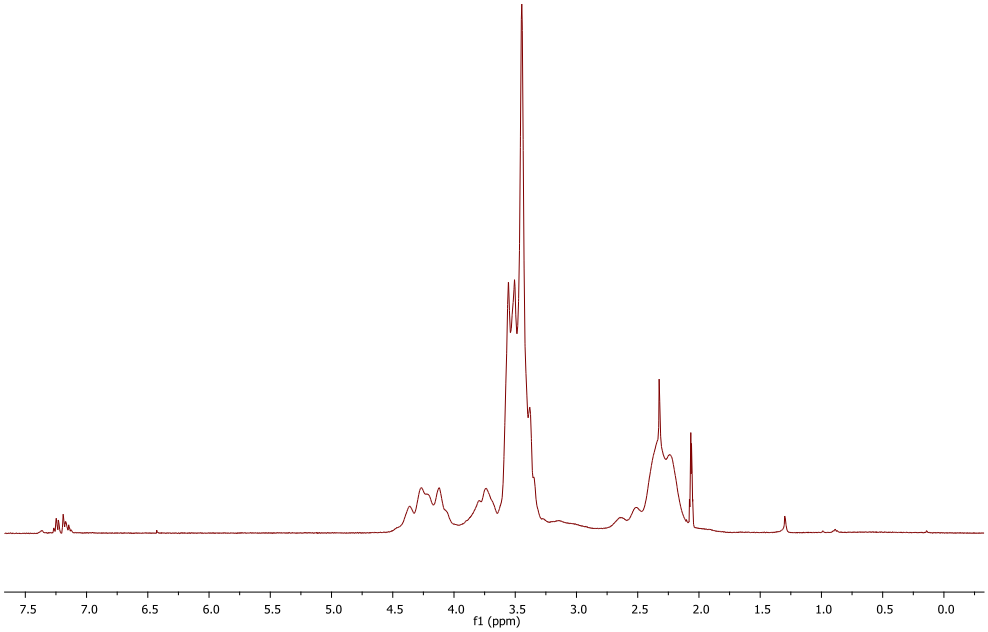

b) Gantrez-Mannosamine

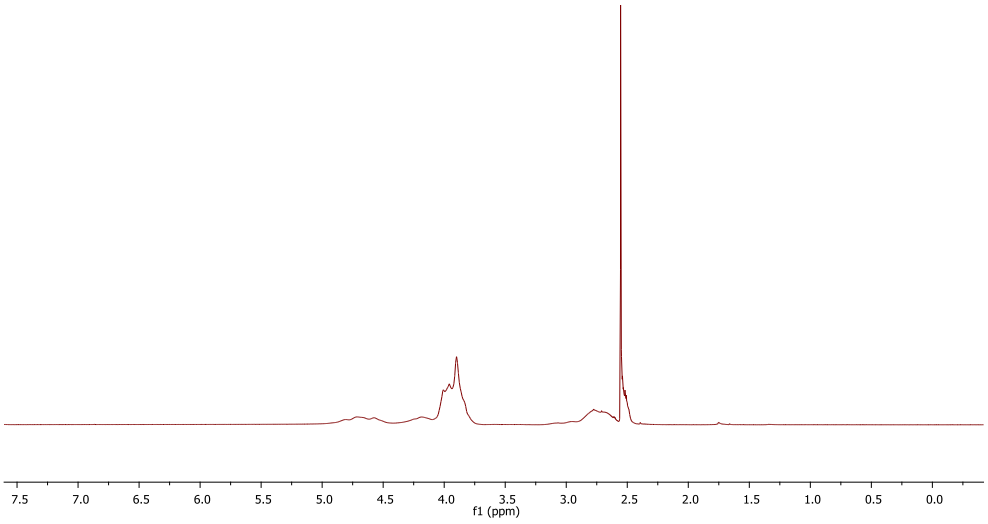

Figure 4S. ^{1}H-NMR spectra from Gantrez® AN and the conjugate between this copolymer and mannosamine (GM).

References

1. Benson JR, Hare PE. O-phthalaldehyde: fluorogenic detection of primary amines in the picomole range. Comparison with fluorescamine and ninhydrin. *Proc Natl Acad Sci*. 1975;72(2):619-622. doi:10.1073/pnas.72.2.619
2. Arbos P, Wirth M, Arangoa MA, Gabor F, Irache JM. Gantrez AN as a new polymer for the preparation of ligand-nanoparticle conjugates. *J Control Release*. 2002;83(3):321-330.
3. Doktorovova S, Shegokar R, Martins-Lopes P, Silva AM, Lopes CM, Müller RH, Souto EB. Modified Rose Bengal assay for surface hydrophobicity evaluation of cationic solid lipid nanoparticles (cSLN). *Eur J Pharm Sci.* 2012;45(5):606-612. doi:10.1016/j.ejps.2011.12.016
4. Taylor C, Allen A, Dettmar PW, Pearson JP. Two rheologically different gastric mucus secretions with different putative functions. *Biochim. Biophys. Acta Gen. Subj*. 2004;1674:131-138.
5. Wilcox MD, Van Rooij LK, Chater PI, Pereira de Sousa I, Pearson JP. The effect of nanoparticle permeation on the bulk rheological properties of mucus from the small intestine. *Eur J Pharm Biopharm*. 2015;96:484-487. doi: 10.1016/j.ejpb.2015.02.029